Quantum magnets and glasses

1996 J. Phys.: Condens. Matter 8 9759

(http://iopscience.iop.org/0953-8984/8/48/007)

J. Phys.: Condens. Matter **8** (1996) 9759–9772. Printed in the UK

Quantum magnets and glasses

Thomas F Rosenbaum

The James Franck Institute and Department of Physics, The University of Chicago, Chicago, IL 60637, USA

Received 3 September 1996

Abstract. We explore the behaviour of the dipolar-coupled Ising magnet, $LiHo_xY_{1-x}F_4$, in a transverse magnetic field. The transverse field, applied perpendicular to the Ising axis, introduces quantum channels for relaxation, thereby continuously depressing the spin-ordering temperature to zero. We compare the classical (thermally driven) and the quantum (transverse-field-driven) transitions for both the pure ferromagnet, $LiHoF_4$, and the spin glass, $LiHo_{0.167}Y_{0.833}F_4$, and we discuss the implications of these results for the $T = 0$ disordered ferromagnet ($x = 0.5$). Finally, we contrast these high-resolution studies of model quantum transitions in insulating magnets with the quantum critical behaviour of the highly correlated Mott–Hubbard metals V_2O_3 and $Ni(S, Se)_2$.

1. Introduction

What is the ground state and what is the dynamics of 10^{23} randomly distributed Ising dipoles? It is easy to write down the spin interaction energy: $E_{ij} = s_i s_j J(1 - \cos^2\theta_{ij})/r_{ij}^3$, where $s_i, s_j = \pm 1$ are the Ising spin variables, $J = g^2\mu_B^2$ is the coupling constant, θ_{ij} is the angle formed by the Ising axis and the vector connecting the spins, and r_{ij} is the distance between spins. But it is difficult to solve for the lowest-energy state because the $1/r^3$ dependence is long range, involving dipoles well beyond nearest neighbours, and the angular dependence introduces competing ferromagnetic and antiferromagnetic ($55^\circ \leqslant \theta_{ij} \leqslant 125^\circ$) interactions. In the concentrated limit, Luttinger and Tisza [1] showed that an underlying lattice contains the requisite information to establish true long-range magnetic order. At sufficient dilution, however, the dipoles have many sites to choose from; they sit essentially randomly in space, and the possibility arises for glassy behaviour [2].

We have studied just such a model dipolar system and find with increasing dilution a crossover from pristine ferromagnet to reduced-moment ferromagnet to magnetic glass [3]. $LiHo_xY_{1-x}F_4$ is an isostructural dilution series where magnetic Ho^{3+} and non-magnetic Y^{3+} ions randomly occupy the rare-earth (R) sites in the body-centred tetragonal $LiRF_4$ lattice [4]. The single-ion anisotropy is Ising with the moments ($\mu_{eff} = 7\mu_B$) derived from the ground-state doublet of Ho^{3+} lying parallel to the c-axis. The dominant interaction between moments is dipolar, as directly demonstrated by neutron diffraction [3, 5]. The pure compound, $LiHoF_4$, is a ferromagnet with an essentially perfect mean-field transition at $T_c = 1.53$ K [6]. The mean-field behaviour to within logarithmic corrections reflects the long-range nature of the dipole–dipole interaction, while the relatively low-energy scale for the transition reflects the weakness of the dipolar coupling compared to the usual exchange mechanism.

0953-8984/96/489759+14$19.50

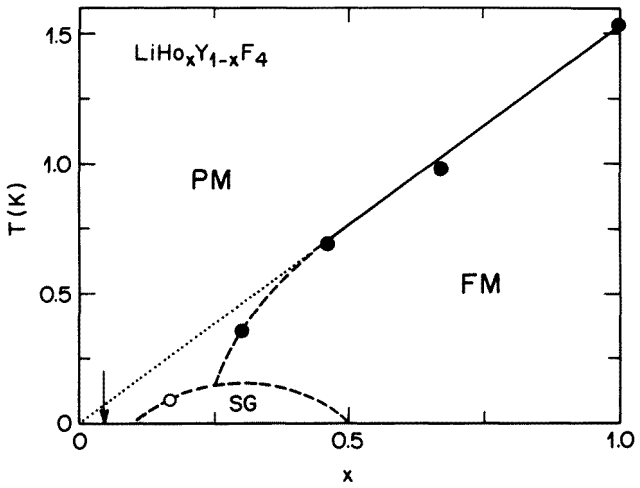

Figure 1. The phase diagram as a function of dipole concentration x for the Ising magnet/glass, $LiHo_xY_{1-x}F_4$. PM = paramagnet, FM = ferromagnet, SG = spin glass. In the dilute limit, the system only freezes for temperature $T = 0$ (arrow). (From reference [3].)

As can be seen in the phase diagram of figure 1, the Curie temperature is depressed linearly with dipole concentration down to at least 50% dilution: $T_c(x) = xT_c(x = 1)$. With only 30% of the sites occupied by magnetic dipoles, the long-range ferromagnetic order survives, but there are decoupled regions of unaligned spins yielding an incomplete global magnetic moment [7]. By 17% dipole (Ho) concentration, the disorder (from dilution) and frustration (from competing interactions) dominate and a classic spin-glass transition ensues with a transition temperature $T_g = 0.13$ K [8]. Finally, at the lowest dipole concentrations, the spin glass is replaced by a qualitatively different ground state which does not appear to freeze at finite temperature [9], which we have coined a 'decoupled cluster glass'.

In this discussion, we will concentrate on the contrasting behaviour of the pure ferromagnet, $x = 1$, and the spin glass, $x = 0.167$. True to the title, however, it is the quantum nature of the problem which most interests us. The classical, thermally driven transitions in the Ising magnet/glass $LiHo_xY_{1-x}F_4$ can be converted into quantum transitions driven by a transverse magnetic field H_t at $T = 0$. The transverse field, applied perpendicular to the Ising axis, mixes the eigenfunctions of the ground-state Ising doublet with the previously inaccessible excited states, leading to a rapid increase in the relaxation due to the existence of new tunnelling modes. This effect can be seen most clearly in the spin glass which is characterized by a broad spectrum of relaxation times. We plot in figure 2 the dissipative response as a function of frequency f at a temperature 35% above the glass transition. The application of even a few kOe of transverse field radically affects the time-scale of the response; the peak frequency, f_p, of the imaginary part of the susceptibility, $\chi''(f)$, increases by two orders of magnitude by 6 kOe. Furthermore, it is the long-time (low-frequency) modes which are shorted out by tunnelling. This is demonstrated in the scaling plot of figure 3, where it is the low-frequency tails of $\chi''(f)$ which are preferentially suppressed.

A complete suppression of freezing can be obtained for laboratory values of H_t. It is then possible to investigate quantitatively with exquisite resolution the influence of either classical or quantum fluctuations on the critical behaviour in the same physical system.

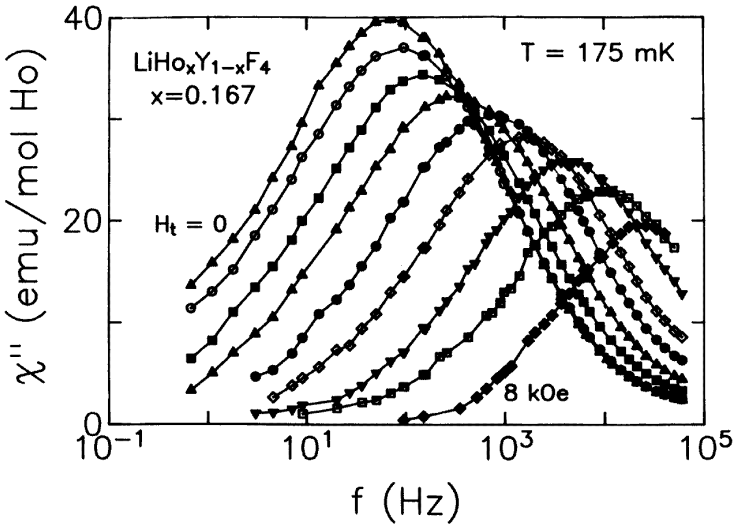

Figure 2. The dissipative response over many decades in frequency for the spin glass at $T > T_g$ for a series of transverse fields H_t in 1 kOe intervals. The glassy response speeds up dramatically as H_t introduces new quantum routes to relaxation. (From reference [8].)

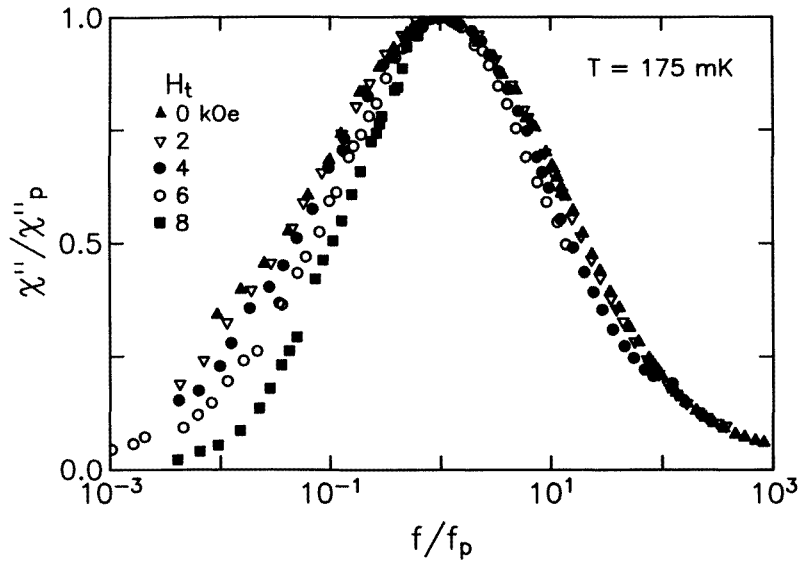

Figure 3. The curves of figure 2 scaled by peak frequency and peak height. The long-time modes are preferentially suppressed by the increased tunnelling in a transverse field.

Moreover, we can independently introduce the variables of disorder and frustration simply by moving across the phase diagram of figure 1.

Single crystals of $LiHo_xY_{1-x}F_4$ provide a model system for studying quantum critical behaviour in clean, insulating magnets and magnetic glasses. There is no confusion introduced by charge carriers—the peculiar mix of the spin and charge degrees of freedom

in transition metal oxides [10], the apparent 'non-Fermi-liquid' behaviour of highly correlated f-electron compounds [11, 12], the unusual normal-state properties of the high-T_c superconducting cuprates [13–16]—where, in each case, the remarkable properties have been ascribed to the proximity of a $T = 0$ quantum critical point. On the other hand, without charge carriers, there cannot be these types of remarkable properties! Hence, we present as well the quantum critical behaviour of the $T = 0$ pressure-driven transitions from spin-density-wave to paramagnet in the correlated metal vanadium sesquioxide and from insulator to metal in the Mott–Hubbard compound $Ni(S, Se)_2$. In both these cases, the physics is sufficiently complicated that it is not possible to independently control the physical variables and it is difficult to model the behaviour from first principles (cf. $LiHoF_4$). Nonetheless, we are able to probe the singular mixture of statics and dynamics stirred up by quantum fluctuations.

2. The model magnet in a transverse field

$LiHoF_4$ in an external field H_t is the experimental realization of the simplest quantum spin model, namely the Ising magnet in a transverse magnetic field. The corresponding Hamiltonian is

$$H = \sum_{i,j}^{N} J_{ij}\sigma_i^z\sigma_j^z - \Gamma\sum_{i}^{N}\sigma_i^x \tag{1}$$

where the σs are Pauli spin matrices, the J_{ij}s are longitudinal couplings, and Γ is a transverse field. Since the commutator $[H, \sigma^z]$ is finite when $\Gamma \neq 0$, zero-point fluctuations are germane at low temperatures. These fluctuations increase with Γ, which tunes an order–disorder transition at $T = 0$.

The magnetic field H_t is applied perpendicular to the easy (c-) axis for the Ho spins. The first excited crystal-field level is 9.4 K above the ground-state doublet; at the low temperatures ($0.025 < T < 2$ K) of our experiments, only the Ising doublet is appreciably populated. It then can be split in a continuous fashion with great precision by the laboratory field H_t. The splitting Γ plays the role of the transverse field in equation (1), while the doublet plays the role of the spin-1/2 eigenstates.

We map out the transverse-field–temperature phase diagram for the pure Ising ferromagnet in figure 4 [17]. The phase boundary follows from the divergence of the linear susceptibility, $\chi'(T, H_t)$, in precise scans of both temperature and transverse magnetic field. We illustrate such scans in reduced temperature and reduced field at the same point in the phase diagram ($T_c \sim 0.1$ K and $H_t^c \sim 49$ kOe, respectively) in figure 5. As expected, the critical exponent (slope) is the same, but varying the transverse field permits higher-resolution studies of the critical point, closer than 10^{-3} in the reduced variable.

The critical exponent for the divergence of the susceptibility retains its mean-field value, $\gamma = 1$ (within error bars), at all temperatures studied, down to 3% of $T_c(H_t = 0)$. Hence, we conclude that both the classical and quantum limits in $LiHoF_4$ exhibit mean-field character. This observation verifies the long-standing and elegant theory [18] identifying ($T = 0$) quantum phase transitions in d dimensions with thermal phase transitions in $d + 1$ dimensions.

Upon observing mean-field-like critical behaviour in both the classical and quantum limits in $LiHoF_4$, it is natural to ask whether the entire phase diagram can be explained in terms of mean-field theory. The exact mean-field phase boundary can be calculated by

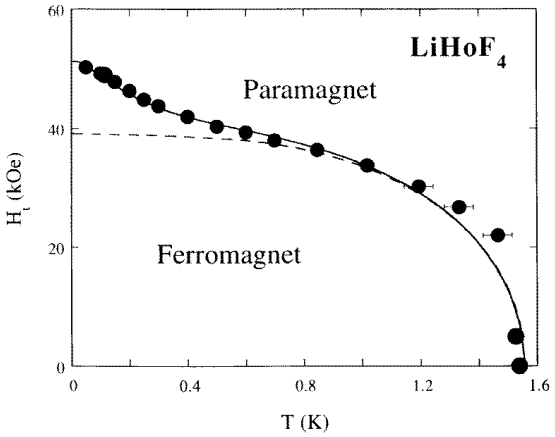

Figure 4. The experimental phase boundary (filled circles) for the pure ferromagnet in the transverse-field–temperature plane. The dashed line is from a mean-field theory including only the electronic spin degrees of freedom; the solid line is from a full mean-field theory incorporating the nuclear hyperfine interaction (equation (2)). Both theories have the same two fitting parameters. (From reference [17].)

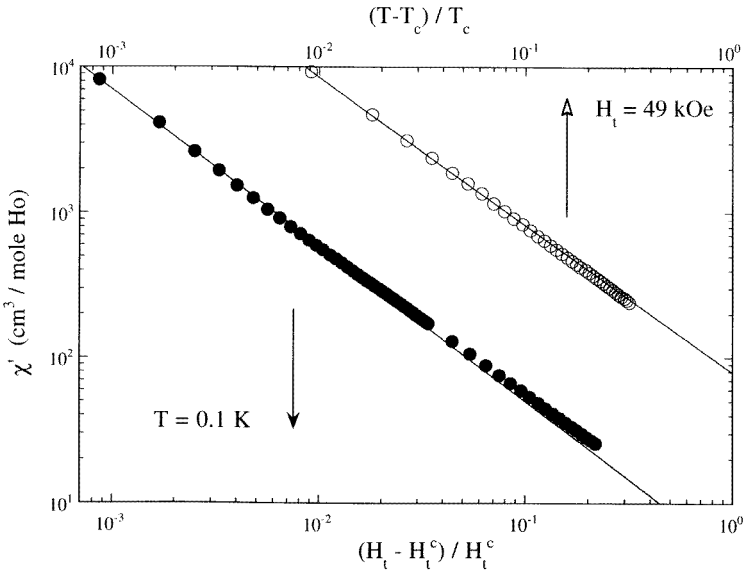

Figure 5. Mean-field critical behaviour of the magnetic susceptibility in the $T \to 0$ limit as functions of reduced temperature (open circles, $T_c = 0.114$ K, $H_t = 49.0$ kOe) and reduced transverse field (filled circles, $H_t^c = 49.3$ kOe, $T = 0.100$ K). (From reference [17].)

solving the Hamiltonian for a single Ho^{3+} ion ($J = 8, I = 7/2$) self-consistently:

$$H = V_c - g_\perp \mu_B H_t \hat{J}_x + A(\hat{I}\hat{J}) - 2J_0\langle \hat{J}_z \rangle \hat{J}_z \tag{2}$$

where V_c represents the zero-field crystal-field operator [19], $g_\perp$ is the transverse g-factor, A is the hyperfine coupling strength, and J_0 is an averaged spin–spin longitudinal coupling constant. The hyperfine term arises from the interaction of the Ho nuclear spins with the

electronic states through a core polarization effect [4, 20]. For $LiHoF_4$, both heat capacity [4] and hyperfine resonance [21] measurements at low T give $A = 0.039$ K $= (A_\parallel)(g/g_\parallel)$, where $A_\parallel = 0.43$ K, the Landé g-factor $g = 1.25$, and the ground-state longitudinal g-factor $g_\parallel = 13.8$.

A solution for T_c as a function of H_t is found by fixing H_t and then calculating $\langle \hat{J}_z \rangle$ self-consistently, starting at a high temperature and then decreasing T in small steps until a non-zero (spontaneous) magnetization is observed. The hyperfine interaction effectively mixes the nuclear and electronic eigenstates together; therefore, the solution proceeds by diagonalizing equation (2) in a (136×136) eigenfunction space (17 crystal-field states $\times$ 8 nuclear states). The solution is shown in figure 4 as the solid line, providing an excellent account of the experimental data. We find best-fit values $J_0 = 0.0270 \pm 0.0005$ K and $g_\perp = 0.74 \pm 0.04$. The value $J_0 = 0.0270$ K $\simeq 2T_c(H_t = 0)(g/g_\parallel)^2$. The experimentally determined value of $g_\perp$ is remarkably close to the single-ion Landé g-factor given the large uncertainty in the matrix elements of J_x which connect the ground-state and excited-state crystal-field levels. These matrix elements are calculated from the eigenstates of V_c and depend on measurements which not only contain statistical errors $\geqslant 25\%$, but are interpolated from the dilute limit (lightly doped $LiYF_4$) [19].

We can illuminate the underlying physics and recover the more conventional mean-field form of the phase diagram by fixing J_0 and $g_\perp$ to their best-fit values and setting $A = 0$ in equation (2). Solving self-consistently for the magnetization gives the dashed line in figure 4. At high temperature, $\boldsymbol{J}$ is the only pertinent quantum number. At low T, however, the eigenstates of $\hat{I}$ and $\hat{J}$ are slaved together, and an effective composite spin $(\boldsymbol{I} + \boldsymbol{J})$ raises the transverse-field scale required to destroy the ferromagnetic state. Hence, it is clear that the upturn in the phase boundary for $T < 0.6$ K results directly from the inclusion of the well-known Ho^{3+} hyperfine term in the Hamiltonian.

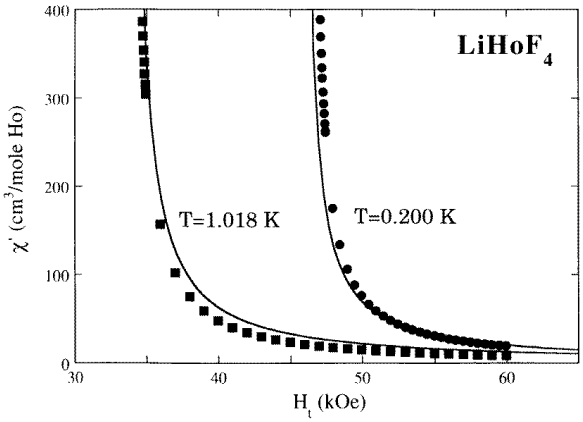

Figure 6. The transverse-field dependence of the susceptibility in the paramagnet for two temperatures. The solid line is a first-principles calculation with parameters fixed by the fit to the phase boundary of figure 4. (From reference [17].)

As a further test that the full mean-field Hamiltonian of equation (2) is an accurate description of the physics, we use it to calculate the susceptibility $\chi'(H_t)$ of $LiHoF_4$ in the paramagnet. The calculation is performed by adding a small ($\sim 10^{-3}$ Oe) longitudinal field h_z to the Hamiltonian and solving self-consistently for the magnetization M_z with no floating parameters. The susceptibility χ' is then M_z/h_z, where we have checked explicitly

that no higher-order terms in h_z are present. We plot in figure 6 the measured $\chi'(H_t)$ at two temperatures, one in the classical regime ($T = 1.018$ K) and one in the quantum regime where the hyperfine term has a large effect ($T = 0.200$ K), together with the calculated values of χ'. The congruence of experiment and theory shows that a complete mean-field treatment can predict accurately both the functional form and the absolute value of the susceptibility as it falls off in the paramagnet with increasing transverse field.

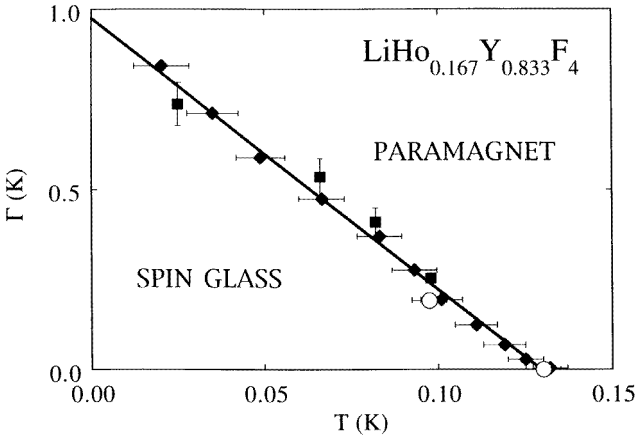

Figure 7. The phase diagram for the spin glass in a transverse field. Filled diamonds follow from low-frequency measurements of χ_1'', open circles from the high-frequency response, and filled squares from the $f \to 0$ divergence of χ_3'. (Following reference [22].)

3. From classical to quantum glass

We plot in figure 7 the phase diagram analogous to figure 4 for the Ising spin glass, $LiHo_{0.167}Y_{0.833}F_4$. The different symbols represent different experimental signatures of the onset of glassiness, including the low-frequency dissipative response [8], an unexpected high-frequency characteristic also seen in supercooled liquids [22], and the divergence of the static non-linear susceptibility [23]. The complexity of spin-glass interactions and order rules out any attempt at simple mean-field modelling, but it is clear from inspection that thermal fluctuations ($T_g = 0.13$ K) are far more efficient than quantum fluctuations ($\Gamma_g = 0.98$ K) in destroying the ordered state.

As in the case of the pure $LiHoF_4$, we should like to compare the critical behaviour in the classical and quantum limits. By contrast to the ferromagnet, the spin glass has zero net magnetization, making the linear magnetic susceptibility an unsatisfactory critical parameter. The non-linear susceptibility, however, represents a higher-order correlation function and it is believed to couple to the spin-glass order parameter. The divergence of the lowest-order non-linear susceptibility, χ_3', at the classical spin-glass transition is seen clearly in figure 8, as is the peaked, but non-diverging form of χ_1' plotted on the same axis.

We follow the static critical response of the non-linear susceptibility down to low temperature and high transverse field in figure 9. The sharp divergence measured in the classical limit becomes suppressed and effectively disappears as $T \to 0$. By $T = 0.025$ K, χ_3' only shows a flat maximum. The (unscaled) overlap of the $\chi_3'(H_t)$ data above 12 kOe defines the regime where the splitting Γ of the Ising doublet dominates any thermal or

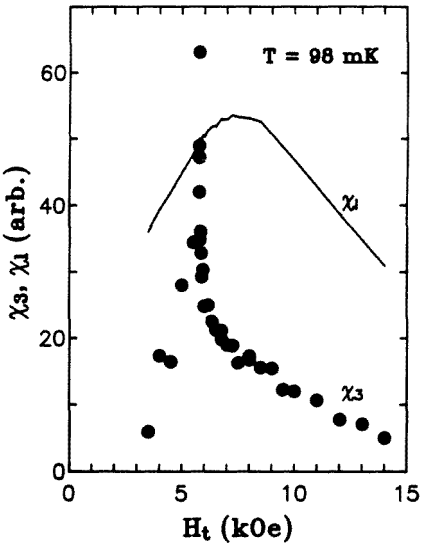

Figure 8. Divergence of the non-linear susceptibility χ_3 at the classical spin-glass transition. The linear susceptibility χ_1 is rounded at the 1.5 Hz measuring frequency.

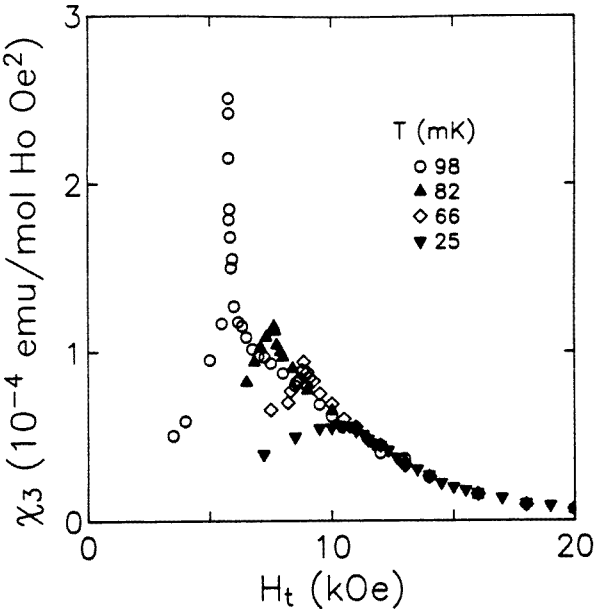

Figure 9. The evolution of the non-linear susceptibility at the spin-glass transition as $T \rightarrow 0$. The clear divergence in the classical limit is quenched in the low-T, large-H_t quantum limit. (Following reference [23].)

spin–spin interaction energy.

The quenching of the divergence of the non-linear susceptibility in the quantum limit raises the question of whether a well-defined spin-glass transition still occurs. We show

in figure 10 simultaneous measurements of the imaginary part of the linear susceptibility in the zero-frequency limit. There is a clear dynamical signature of the transition at all temperatures, even sharpening at low T and high H_t. The large dissipation at low transverse field is due to the development of a flat, frequency-independent tail in $\chi_1''(f \to 0)$ [8], which, by the fluctuation-dissipation theorem, corresponds to characteristic $1/f$ noise in the spin-glass magnetization [24].

Mean-field treatments of both infinite-range quantum Ising [25] and quantum rotor [26] spin glasses predict unusual behaviour for the non-linear susceptibility at the $T = 0$ transition, but retain its divergence. Specifically, they give $\gamma_{eff} = 1/2$ and a phase boundary $\Gamma_g(T) - \Gamma_g(T = 0) \sim T^2$ at low T. Our experiment yields $\gamma_{eff} < 1/2$ at all T measured, with an essentially linear phase boundary. If we attempt to fit the weak divergence of χ_3 with transverse field to a critical form for the lower temperatures, then we are faced with the rare situation of a progressively decreasing, temperature-dependent critical exponent, γ_{eff}, indistinguishable from zero by $T = 0.025$ K. More likely, the $T = 0$ quantum spin-glass transition is first order. While the non-ergodicity of the spin-glass state precludes the standard test of hysteresis at a first-order transition, this hypothesis is consistent with both the abrupt onset of linear dissipation and the absence of a pre-transitional divergence of χ_3 (and the spin-glass correlation length). Moreover, in quantum systems of finite size, first-order transitions in the form of level crossings are the rule rather than the exception. If low-dimensional systems serve as a guide [27], then level crossings associated with strong but relatively rare bonds dominate the transition into the spin-glass state.

4. Implications

The classical and quantum limits are strikingly similar in the pure, dipolar-coupled, Ising ferromagnet; it would be difficult for them to be more dissimilar in the dipolar-coupled, Ising spin glass. Yet, there is an intermediate case: the full-moment, but disordered ferromagnets with dipole concentrations between 0.5 and 1. With the quantitative understanding and modelling tools that we have developed for the pure ferromagnet in a transverse magnetic field, it should be possible to use $LiHoF_4$ as a quantitative benchmark for the effects of disorder on a quantum critical point. Will the quantum phase transition in $LiHo_{0.5}Y_{0.5}F_4$ remain continuous and mean-field-like or will it be first order? Is it the disorder or the frustration which plays the key role at the $T = 0$ spin-glass transition? To that end, it is possible as well to probe the effects of frustration alone—no disorder—through analogous transverse-field studies of pure, layered antiferromagnets such as $LiErF_4$. Finally, it is not the phase boundary itself which holds all of the salient information about the influence of quantum mechanics. It should be possible to compare thermal (T) and quantum (H_t) 'excursions' deep in the ordered state, of special interest for the tunable tunnelling of domain walls in the ferromagnet and the exploration of the complicated free-energy surface in the spin glass.

5. Correlated metals

Barely delocalized and strongly correlated electrons diffusing in a disordered medium are prone to exhibiting unusual magnetic order. This tendency towards reduced-moment magnetism in the metal certainly complicates models of the Mott–Hubbard metal–insulator transition. It also offers a unique opportunity to study the behaviour of an itinerant-fermion system in the immediate vicinity of a quantum critical point. Vanadium sesquioxide is one

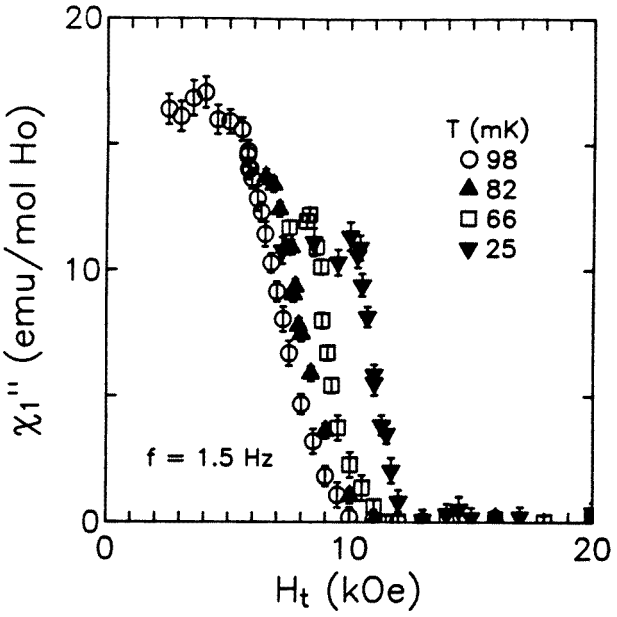

Figure 10. Behaviour corresponding to figure 9 in the dissipative response. A clear dynamical signature of the spin-glass transition remains, even sharpening in the quantum limit. (Following reference [23].)

of these select systems where a $T = 0$ magnetic instability can be accessed using modest laboratory pressures [10]. The low-temperature metal has an incommensurate, spiral spin-density wave which partially gaps the Fermi surface and which bears no obvious relationship to the antiferromagnetism in the insulator [28]. The magnetism in the metal is unstable with respect to the application of modest hydrostatic pressures, which introduces a new $T = 0$ phase boundary between antiferromagnetic metal and paramagnetic (Brinkman–Rice) metal [29].

Building on the work of Hertz [30], Millis [31] has made quantitative predictions for the behaviour of the magnetic phase boundary at the approach to the quantum critical point. His prediction that the magnetic ordering temperature should approach zero as $\{(P - P_c)/P_c\}^{z/(z+1)}$, where z is the dynamical exponent, works well for the ferromagnet $ZrZn_2$ [32] with $z = 3$, but does not appear to account for the data on the antiferromagnet ($z = 2$). In the case of the heavy-fermion compound Au-doped $CeCu_6$ [11], pressure depresses the Néel temperature linearly to zero, as opposed to the predicted sublinear dependence. For $P > P_c$, this system also displays robust 'non-Fermi-liquid' behaviour in the susceptibility and the specific heat.

On a coarse pressure scale, compressed $V_{2-y}O_3$ similarly appears to approach its $T = 0$ antiferromagnetic instability in linear fashion [10]. However, the resistivity and magnetic susceptibility measurements of figure 11 reveal a distinct downward curvature in the close vicinity of P_c. The influence of the quantum critical point has emerged, but these preliminary data [33] are not sufficiently good to test whether the sublinear dependence of T_N on reduced pressure is actually described by a 2/3 power. We note that the assignment of $P_c = 7.3$ kbar is corroborated by independent measurements of the evolution of the magnetic moment with pressure [33]. The questions remain open as to whether (i) the d electrons of V also exhibit

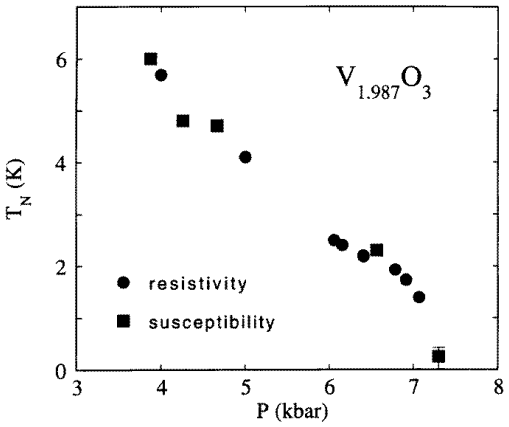

Figure 11. The phase boundary for the $T = 0$ pressure-driven transition from spin-density wave to paramagnet in highly correlated, metallic vanadium sesquioxide. Close to $P_c = 7.3$ kbar, the influence of the quantum critical point appears to manifest itself in the downward curvature of $T_N(P)$.

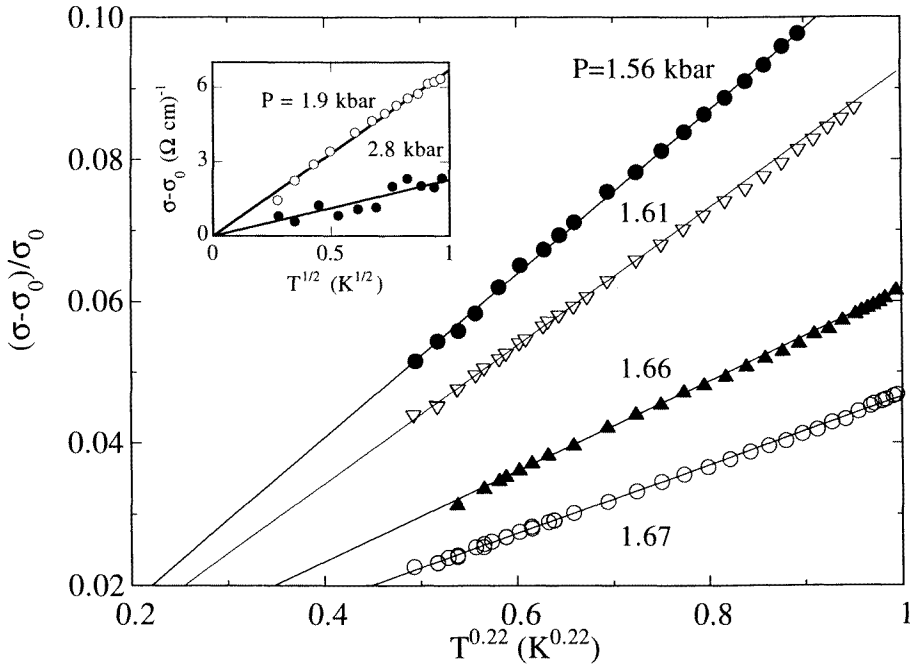

Figure 12. Far above the critical pressure, $P_c = 1.51$ kbar, for the Mott–Hubbard metal–insulator transition in $NiS_{1.56}Se_{0.44}$, the conductivity σ exhibits the usual $T^{1/2}$-form characteristic of electron–electron interactions in the presence of disorder (inset). The increasing slope with decreasing P reflects an effective-mass enhancement at the approach to the transition. For P close to P_c an unusual new functional form, $T^{0.22}$, appears for $T < 1$ K, representing the dynamical signature of the $T = 0$ Mott–Hubbard critical point. (Following reference [34].)

'non-Fermi-liquid' characteristics for $P > P_c$, or whether the f electrons of Ce and U are uniquely so qualified, and (ii) whether such unconventional behaviour is tied to deviations from the Millis predictions for the critical form for the magnetic phase boundary.

The intertwined dynamical and static response at a quantum critical point also comes to the fore in our studies of the $T = 0$ metal–insulator transition in $Ni(S, Se)_2$. This solid solution of the semiconductor nickel disulphide and the metal nickel diselenide is one of the few highly correlated, Mott–Hubbard systems without a strong first-order structural distortion cutting off the critical behaviour at the metal–insulator transition. We start with $NiS_{1.56}Se_{0.44}$ crystals just on the insulating side of the boundary and drive the system metallic with pressure [34]. The static critical behaviour, $\sigma(T = 0) \sim \{(P - P_c)/P_c\}^{\mu}$ with $\mu = 1.1 \pm 0.2$ is unsurprising, being common to all Anderson transitions save that in uncompensated Si [35]. Rather, it is the dynamics, again right at the $T = 0$ critical point, which reveals a telltale signature. We focus in figure 12 on the low-temperature behaviour of the conductivity for pressures very near the $T = 0$ metal–insulator transition. At pressures more than 0.2 kbar above the transition we observe the usual $T^{1/2}$-form of the conductivity characteristic of electron–electron interactions in the presence of disorder [36]. However, for $P \sim P_c$, the influence of the quantum critical point becomes apparent. A new functional form, $\sigma - \sigma(0) \sim T^{0.22}$, describes best the dynamical (finite-T or finite-ω) response. This unusual exponent follows either from a simple two-parameter least-squares fit (0.20 ± 0.07) for $0.035\ \text{K} < T < 0.800\ \text{K}$ or more precisely (0.22 ± 0.02) from a dynamical scaling analysis [37] whereby we collapse the transport data for the six pressures closest to P_c and $T < 1$ K onto a universal scaling curve [34].

6. Conclusions

The $T = 0$ metal–insulator transition in disordered systems is the best known and most studied quantum phase transition. In a few special cases, strong charge and spin correlations coexist with an effectively continuous transition and it remains possible to explore the nature of the critical point through the appropriate combination of static and dynamic probes. Nonetheless, the field has been handicapped by the difficulty of readily identifying a suitable order parameter. As an alternative, one can investigate the $T = 0$ physics of spin systems. Magnetic phase transitions in the classical limit have been investigated extensively, and as thermal fluctuations give way to quantum fluctuations, one expects that the generalized magnetic susceptibility will continue to reveal the critical behaviour. When charge carriers are present, the $T = 0$ critical point, combined with pronounced interactions of electronic and/or magnetic character, gives rise to novel low-temperature phases. It is hard to know what other than critical exponents can be theoretically modelled, but it is clear that high-resolution measurements near the $T = 0$ transition need to be combined with studies of the quantum-to-classical crossover. Finally, model systems such as the clean, insulating magnet $LiHo_xY_{1-x}F_4$ in a transverse magnetic field provide the means to contrast the influence of thermal and quantum fluctuations in the same physical system. With varying dipole concentration (x) as an extra degree of freedom, this material has the added potential to establish the underpinnings for a quantitative understanding of the role of disorder and/or frustration at the quantum critical point.

Acknowledgments

The experiments on $Li(Ho, Y)F_4$ were conceived and performed with Gabriel Aeppli. The contributions of D H Reich, W Wu, and D Bitko have been indispensable. The work reported here on V_2O_3 and $Ni(S, Se)_2$ has been led by A Husmann and D S Jin, with crystals and inspiration from J M Honig. I thank them and my many collaborators whose names can be found in the references. The work at the University of Chicago was supported by the MRSEC Program of the National Science Foundation under Award No DMR-9400379 and by NSF Grant No DMR95-07873.

References

[1] Luttinger J M and Tisza L 1946 *Phys. Rev.* **70** 954
[2] Aharony A and Stephen M J 1981 *J. Phys. C: Solid State Phys.* **14** 1665
[3] Reich D H, Ellman B, Yang J, Rosenbaum T F, Aeppli G and Belanger D P 1990 *Phys. Rev.* B **42** 4631
[4] Keller C and Schmutz H 1965 *J. Inorg. Nucl. Chem.* **27** 900
Mennenga G, de Jongh L J and Huiskamp W J 1984 *J. Magn. Magn. Mater.* **44** 59
[5] Als-Nielsen J 1976 *Phys. Rev. Lett.* **37** 1161
[6] Ahlers G, Kornblit H and Guggenheim H J 1975 *Phys. Rev. Lett.* **34** 1227
[7] Kjaer K, Als-Nielsen J, Laursen I and Krebs Larsen F 1989 *J. Phys.: Condens. Matter* **1** 5743
[8] Wu W, Ellman B, Rosenbaum T F, Aeppli G and Reich D H 1991 *Phys. Rev. Lett.* **67** 2076
[9] Reich D H, Rosenbaum T F and Aeppli G 1987 *Phys. Rev. Lett.* **59** 1969
[10] Carter S A, Rosenbaum T F, Honig J M and Spalek J 1991 *Phys. Rev. Lett.* **67** 3440
Carter S A, Rosenbaum T F, Metcalf P, Honig J M and Spalek J 1993 *Phys. Rev.* B **48** 16 841
[11] von Löhneysen H *et al* 1994 *Phys. Rev. Lett.* **72** 3262
Bogenberger B and von Löhneysen H 1995 *Phys. Rev. Lett.* **74** 1016
[12] For a review, see
Maple M B *et al* 1995 *J. Low Temp. Phys.* **99** 223
[13] Chakravarty S, Halperin B I and Nelson D R 1989 *Phys. Rev.* B **39** 2344
[14] Sachdev S and Ye J 1992 *Phys. Rev. Lett.* **69** 2411
Chubukov A and Sachdev S 1993 *Phys. Rev. Lett.* **71** 169
Sokol A and Pines D 1993 *Phys. Rev. Lett.* **71** 2813
Sandvik A W and Scalapino D J 1994 *Phys. Rev. Lett.* **72** 2777
Sandvik A W and Vekic M 1995 *Phys. Rev. Lett.* **74** 1226
[15] Keimer B, Birgeneau R J, Cassanho A, Endoh Y, Erwin R W, Kastner M A and Shirane G 1991 *Phys. Rev. Lett.* **67** 1930
Hayden S M, Aeppli G, Mook H, Rytz D, Hundley M F and Fisk Z 1991 *Phys. Rev. Lett.* **66** 821
[16] Imai T, Slichter C P, Yoshimura K and Kosuge K 1993 *Phys. Rev. Lett.* **70** 1002
Imai T, Slichter C P, Yoshimura K, Katoh M and Kosuge K 1993 *Phys. Rev. Lett.* **71** 1254
[17] Bitko D, Rosenbaum T F and Aeppli G 1996 *Phys. Rev. Lett.* **77** 940
[18] Suzuki M 1976 *Prog. Theor. Phys.* **56** 1454
Oitmaa J and Coombs G J 1981 *J. Phys. C: Solid State Phys.* **14** 143
[19] Hansen P E, Johansson T and Nevald R 1975 *Phys. Rev.* B **12** 5315
[20] Andres K 1973 *Phys. Rev.* B **7** 4295
[21] Magarinõ J *et al* 1980 *Phys. Rev.* B **21** 18
[22] Bitko D, Menon N, Nagel S R, Rosenbaum T F and Aeppli G 1996 *Europhys. Lett.* **33** 489
[23] Wu W, Bitko D, Rosenbaum T F and Aeppli G 1993 *Phys. Rev. Lett.* **71** 1919
[24] Ocio M, Bouchiat H and Monod P 1985 *J. Physique Lett.* **46** L647
Fisher D and Huse D 1986 *Phys. Rev. Lett.* **56** 1601
Israeloff N E, Alers G B and Weissman M B 1991 *Phys. Rev.* B **44** 12 613
[25] Miller J and Huse D A 1993 *Phys. Rev. Lett.* **70** 3147
[26] Ye J, Sachdev S and Read N 1993 *Phys. Rev. Lett.* **70** 4011
[27] Bray A J and Moore M A 1980 *J. Phys. C: Solid State Phys.* **13** L655
McCoy B M and Wu T T 1968 1992 *Phys. Rev.* **176** 631
Fisher D S *Phys. Rev. Lett.* **69** 534

[28] Bao W, Broholm C, Carter S A, Rosenbaum T F, Aeppli G, Metcalf P, Honig J M, Spalek J and Trevino S 1993 *Phys. Rev. Lett.* **71** 766
[29] For a recent review, see
Rosenbaum T F 1995 *The Metal–Nonmetal Transition Revisited* ed P P Edwards and C N Rao (London: Taylor and Francis) p 105
[30] Hertz J A 1976 *Phys. Rev.* B **14** 1165
[31] Millis A J 1993 *Phys. Rev.* B **48** 7183
[32] Grosche M 1994 *PhD Thesis* Cambridge University
[33] Husmann A *et al* 1996 to be published
[34] Husmann A, Jin D S, Zastavker Y V, Rosenbaum T F, Yao X and Honig J M 1996 at press
[35] See, for example,
Lee P A and Ramakrishnan T V 1985 *Rev. Mod. Phys.* **57** 287
and
Belitz D and Kirkpatrick T R 1994 *Rev. Mod. Phys.* **66** 261
[36] Altshuler B L, Aronov A G and Lee P A 1980 *Phys. Rev. Lett.* **44** 1288
Rosenbaum T F, Andres K, Thomas G A and Lee P A 1981 *Phys. Rev. Lett.* **46** 568
[37] Wegner F J 1976 *Z. Phys.* B **25** 327
Finkel'stein A M 1983 *Sov. Phys.–JETP* **57** 97
Kirkpatrick T R and Belitz D 1994 *Phys. Rev. Lett.* **73** 862